

# Response Dynamics to Pulsed Perturbations of the Hydrogen Peroxide–Thiosulfate–Cu<sup>2+</sup> Reaction

Oldřich Pešek, Vlasta Kofránková, Lenka Schreiberová, and Igor Schreiber\*

Department of Chemical Engineering & Center for Nonlinear Dynamics of Chemical and Biological Systems, Institute of Chemical Technology, Prague, Technická 5, 166 28 Prague 6, Czech Republic

Received: July 16, 2007; In Final Form: October 29, 2007

The hydrogen peroxide–thiosulfate–Cu<sup>2+</sup> reaction operated in a continuous flow stirred tank reactor is a pH-oscillator known to provide three different steady states, hysteresis, and oscillations. In addition to the various dynamical regimes established earlier, a question arises whether the reaction can be also excitable, whereby the system strongly responds to a small but supercritical external addition of certain chemical species. We carried out experiments aimed at finding excitability and studying response dynamics to single and repeated pulsed perturbations of varying amplitude and period. We found that the reaction displays a remarkable excitatory dynamics when forced. The available mechanism of the reaction involves several adjustable parameters, which need to be tuned so that the model corresponds to experimentally observed bifurcation diagrams. Our experimental findings are compared with numerical calculations, suggesting that the model is far from complete.

## 1. Introduction

Initial research on chemical oscillators and excitable systems was focused on the Belousov–Zhabotinsky reaction<sup>1</sup> and further oscillating reactions,<sup>2</sup> where the autocatalysis is mediated by species containing halogen and where pH is essentially constant. The first inorganic pH oscillating reaction<sup>3</sup> was discovered in 1985 and many other soon followed.<sup>4</sup> In these pH-regulated reactions, the concentration of hydrogen ions plays a critical role in the kinetics of the system.<sup>5</sup> The inlet concentration of hydrogen ions is usually significantly lower and never exceeds that of other reactants. The measured oscillatory change of pH as the reaction proceeds is always large. In particular, the relative change in the concentration of hydrogen ions is dramatic, its effect on the reaction kinetics is extremely high and usually autocatalytic.<sup>6</sup>

pH-oscillators are frequently based on oxidation–reduction reactions. Elements in the groups 14, 15, 16, and 17 support a wide range of oxidation states and their oxidation–reduction reactions often exhibit nonlinear dynamical phenomena.<sup>6–8</sup> Among those, the reaction between hydrogen peroxide and thiosulfate in the presence of diluted sulfuric acid and catalytic amounts of Cu<sup>2+</sup> has been shown to display a rich variety of dynamical regimes.<sup>9</sup> Both hydrogen peroxide and thiosulfate are significant species in the field of chemical oscillations. Oxidation of several compounds by hydrogen peroxide<sup>10–12</sup> exhibits oscillatory and other nonlinear reaction dynamics as well as do reactions, where thiosulfate is oxidized by chlorite,<sup>13</sup> periodate,<sup>14</sup> permanganate,<sup>15</sup> etc.

Orbán and Epstein<sup>9</sup> found that when hydrogen peroxide and thiosulfate are fed into the continuous flow stirred tank reactor (CSTR) together with a catalytic amount of Cu<sup>2+</sup> and solution of sulfuric acid, then after a transient period the reaction system may settle in any of the four regimes: three different steady states and a periodic oscillatory regime. In this work, we focus

on the next nonlinear phenomenon – excitability which is a pronounced but transient oscillatory response to a suitable small perturbation. Excitability<sup>16</sup> implies the system's ability to amplify a small stimulus, typically provided by a pulsed addition of a suitable chemical species. This phenomenon has not been studied so far in this reaction, and therefore it is the subject of this work.

In section 2, we first examine the autonomous dynamics by comparing bifurcation diagrams obtained experimentally with those calculated for a mechanism proposed by Kurin-Csörgei et al.<sup>17</sup> in an effort to optimize adjustable model parameters so that the diagrams match as closely as possible. In section 3, we report experiments on response dynamics to pulsed perturbations applied to various dynamical regimes occurring in the bifurcation diagram, and in section 4, we use the model to simulate the observed response dynamics.

## 2. Dynamic Behavior of the Autonomous System

**Experiments.** In the H<sub>2</sub>O<sub>2</sub>–S<sub>2</sub>O<sub>3</sub><sup>2-</sup>–H<sub>2</sub>SO<sub>4</sub>–Cu<sup>2+</sup> reaction, the three different steady states are distinguished by their pH, which does not significantly vary for any particular steady state with external constraints used in the experiments. The first steady state (SS I) is weakly basic with pH ≈ 8, the second one (SS II) corresponds to a weakly acidic pH ≈ 5, and the third one (SS III) is acidic with pH ≈ 3. The oscillatory regime has amplitude and period depending on external constraints; pH ranges from 3 to 9 and the period is on the order of several minutes.<sup>9</sup> In addition, the dynamical regimes may coexist and the system can be operated in one of these alternative attractors depending on initial state or history. Considering the experimentally observed excitable dynamics in another pH oscillator studied earlier,<sup>18</sup> we can expect that the current system is also excitable with respect to an appropriate external perturbation.

Any dynamical regime, in which the system is found, depends on external constraints such as temperature, or inlet concentrations of reactants. In the region of bistability, it is necessary to

\* Corresponding author. E-mail: schrig@vscht.cz. Telephone: +420 2 2044 3165. Fax: +420 2 2044 4320.

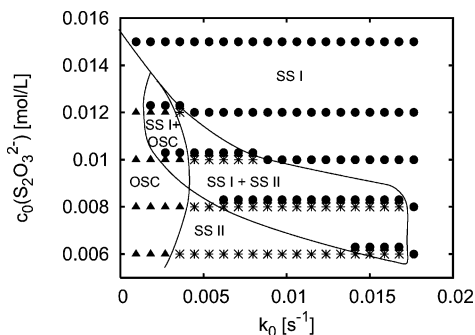


**Figure 1.** Experimental bifurcation diagram in parameter plane  $k_0$ – $c_0(\text{S}_2\text{O}_3^{2-})$ . Conditions:  $c_0(\text{H}_2\text{O}_2) = 0.1$  mol/L,  $c_0(\text{H}_2\text{SO}_4) = 0.001$  mol/L,  $c_0(\text{Cu}^{2+}) = 2.5 \times 10^{-5}$  mol/L. Key: (●) weakly basic SS I; (\*) weakly acidic SS II; (▲) oscillations. Two stacked symbols indicate coexistence of respective regimes. The curves delineating regions of various dynamical modes are drawn to guide the eye. Labels: OSC, oscillations; SS I + SS II, bistability between SS I and SS II; SS I + OSC, bistability between SS I and oscillations.

consider initial state or history of the system, which decides between two possible attractors of the system. The behavior of the system is conveniently summarized in bifurcation diagrams, which were thoroughly examined by Orbán and Epstein.<sup>9</sup> In their work, dynamic modes of the system at fixed temperature 25 °C and inlet concentrations  $c_0(\text{H}_2\text{SO}_4) = 0.001$  mol/L and  $c_0(\text{Cu}^{2+}) = 2.5 \times 10^{-5}$  mol/L are displayed as regions delineated by curves in the plane of two constraints, the inlet concentration of thiosulfate  $c_0(\text{S}_2\text{O}_3^{2-})$  and the flow rate  $k_0$  (reciprocal mean residence time), determined for several fixed values of the inlet concentration of hydrogen peroxide  $c_0(\text{H}_2\text{O}_2)$ . Generally, SS III is found only at very low flow rates or in the batch system, oscillations occur at lower inlet concentrations of thiosulfate and lower flow rates, SS II exists at lower inlet concentrations of thiosulfate but higher flow rates, and finally SS I is found at high inlet concentrations of thiosulfate and high flow rates. With the increasing concentration of hydrogen peroxide, the region of oscillations grows at the expense of the regions of steady states SS I and SS II.

As an initial step in this work, we reproduced some of the diagrams obtained by Orbán and Epstein<sup>9</sup> under the same conditions in an experimental setup described in the next section on pulsed experiments and found consistent results. The bifurcation diagram relevant to our pulsed experiments is shown in Figure 1. This diagram resembles somewhat the classical cross-shaped diagram<sup>19</sup> in that there is a region of coexisting SS I and SS II meeting a region of stable oscillations at a crossover point. The other two regions meeting at this point are the region of the weakly acidic steady-state SS II and the region where the weakly basic steady-state SS I coexists with oscillations. This feature is absent from the classical cross-shaped diagram where the region of a unique SS I occurs instead.

**Model.** We now examine a mechanism of the reaction between hydrogen peroxide and thiosulfate catalyzed by  $\text{Cu}^{2+}$  in the solution of sulfuric acid with the aim of adjusting some uncertain model parameters to obtain a satisfactory agreement between the measured and calculated bifurcation diagrams. The mechanism has been suggested and discussed by Kurin-Csörgei et al.<sup>17</sup> It involves nine reaction steps including three protonation-deprotonation equilibria and nine associated rate equations (Table 1). Some of the rate constants are provided in literature<sup>17</sup> (Table 2), and the rest are adjustable parameters. The mathematical model assumes an isothermal CSTR at 25 °C with ideal

**TABLE 1: Mechanism and Rate Laws of the Reaction<sup>17</sup>**

|   |      |
|---|------|
| $\text{H}_2\text{O}_2 + \text{S}_2\text{O}_3^{2-} \rightarrow \text{HOS}_2\text{O}_3^- + \text{OH}^-$   | (M1) |
| $\text{H}_2\text{O}_2 + \text{HOS}_2\text{O}_3^- \rightarrow 2 \text{HSO}_3^- + \text{H}^+$   | (M2) |
| $\text{S}_2\text{O}_3^{2-} + \text{HOS}_2\text{O}_3^- \rightarrow \text{S}_4\text{O}_6^{2-} + \text{OH}^-$  | (M3) |
| $\text{H}_2\text{O} \rightleftharpoons \text{H}^+ + \text{OH}^-$  | (M4) |
| $\text{H}_2\text{O}_2 \rightleftharpoons \text{H}^+ + \text{HO}_2^-$  | (M5) |
| $\text{H}_2\text{O}_2 + \text{S}_4\text{O}_6^{2-} \rightarrow 2 \text{HOS}_2\text{O}_3^-$   | (M6) |
| $\text{H}_2\text{O}_2 + \text{HSO}_3^- \rightarrow \text{SO}_4^{2-} + \text{H}_2\text{O} + \text{H}^+$  | (M7) |
| $\text{H}_2\text{O}_2 + \text{SO}_3^{2-} \rightarrow \text{SO}_4^{2-} + \text{H}_2\text{O}$   | (M8) |
| $\text{HSO}_3^- \rightleftharpoons \text{H}^+ + \text{SO}_3^{2-}$   | (M9) |
| $r_1 = k_1[\text{H}_2\text{O}_2][\text{S}_2\text{O}_3^{2-}] + k'_1[\text{H}_2\text{O}_2][\text{S}_2\text{O}_3^{2-}][\text{Cu}^{2+}][\text{OH}^-]$ | (R1) |
| $r_2 = k_2[\text{H}_2\text{O}_2][\text{HOS}_2\text{O}_3^-]$   | (R2) |
| $r_3 = k_3[\text{S}_2\text{O}_3^{2-}][\text{HOS}_2\text{O}_3^-] + k'_3[\text{S}_2\text{O}_3^{2-}][\text{HOS}_2\text{O}_3^-][\text{H}^+]$          | (R3) |
| $r_4 = k_4[\text{H}_2\text{O}] - k_{-4}[\text{H}^+][\text{OH}^-]$   | (R4) |
| $r_5 = k_5[\text{H}_2\text{O}_2] - k_{-5}[\text{H}^+][\text{HO}_2^-]$   | (R5) |
| $r_6 = k_6[\text{H}_2\text{O}_2][\text{S}_4\text{O}_6^{2-}] + k'_6[\text{H}_2\text{O}_2][\text{S}_4\text{O}_6^{2-}][\text{OH}^-]$                 | (R6) |
| $r_7 = k_7[\text{H}_2\text{O}_2][\text{HSO}_3^-] + k'_7[\text{H}_2\text{O}_2][\text{HSO}_3^-][\text{H}^+]$  | (R7) |
| $r_8 = k_8[\text{H}_2\text{O}_2][\text{SO}_3^{2-}]$   | (R8) |
| $r_9 = k_9[\text{HSO}_3^-] - k_{-9}[\text{H}^+][\text{SO}_3^{2-}]$  | (R9) |

**TABLE 2: Experimentally Supported Rate Constants of the Mechanism<sup>17</sup> at 25 °C**

|  |  |
|--|--|
| $k_1 = 0.019 \text{ dm}^3 \text{ mol}^{-1} \text{ s}^{-1}$               | $k_7 = 7 \text{ dm}^3 \text{ mol}^{-1} \text{ s}^{-1}$                   |
| $k_4[\text{H}_2\text{O}] = 0.001 \text{ s}^{-1}$                         | $k'_7 = 1.48 \times 10^7 \text{ dm}^6 \text{ mol}^{-2} \text{ s}^{-1}$   |
| $k_{-4} = 1 \times 10^{11} \text{ dm}^3 \text{ mol}^{-1} \text{ s}^{-1}$ | $k_8 = 0.2 \text{ dm}^3 \text{ mol}^{-1} \text{ s}^{-1}$                 |
| $k_5 = 0.022 \text{ s}^{-1}$   | $k_9 = 3 \times 10^3 \text{ s}^{-1}$                                     |
| $k_{-5} = 1 \times 10^{10} \text{ dm}^3 \text{ mol}^{-1} \text{ s}^{-1}$ | $k_{-9} = 5 \times 10^{10} \text{ dm}^3 \text{ mol}^{-1} \text{ s}^{-1}$ |

**TABLE 3: Optimized Rate Constants of the Mechanism<sup>17</sup> at 25 °C**

|   |  |
|---|--|
| $k'_1 = 3 \times 10^8 \text{ dm}^9 \text{ mol}^{-3} \text{ s}^{-1}$ | $k'_3 = 7 \text{ dm}^6 \text{ mol}^{-2} \text{ s}^{-1}$    |
| $k_2 = 0.02 \text{ dm}^3 \text{ mol}^{-1} \text{ s}^{-1}$           | $k_6 = 0.001 \text{ dm}^3 \text{ mol}^{-1} \text{ s}^{-1}$ |
| $k_3 = 1 \text{ dm}^3 \text{ mol}^{-1} \text{ s}^{-1}$              | $k'_6 = 100 \text{ dm}^6 \text{ mol}^{-2} \text{ s}^{-1}$  |

mixing and involves mass balance equations for each reacting species:

$$\frac{dc_i}{dt} = k_0(c_{i0} - c_i) + \sum_j v_{ij}r_j \quad (1)$$

where  $c_i$  is the concentration of the species  $i$  in the reactor,  $k_0$  is the flow rate (reciprocal mean residence time),  $c_{i0}$  is the concentration of the species  $i$  in the inlet,  $v_{ij}$  is the stoichiometric coefficient of species  $i$  in the  $j$ -th reaction, and  $r_j$ 's are reaction rates from Table 1.

In attempt to use the model in simulations of our pulsed experiments, we concentrated on a “best” fit of the experimental bifurcation diagrams presented by Orbán and Epstein.<sup>9</sup> The adjustable parameters are  $k'_1$ ,  $k_2$ ,  $k_3$ ,  $k'_3$ ,  $k_6$ , and  $k'_6$ . There is no clear way how to use an optimization method, such as nonlinear least-squares fit. Moreover, because of uncertainties in the mechanism, using a quantitative procedure would be premature. Instead, we varied the adjustable parameters heuristically and constructed  $k_0$ – $c_0(\text{S}_2\text{O}_3^{2-})$  bifurcation diagrams by means of the software package Cont.<sup>20</sup> These diagrams were compared with the experimental ones and by repeated readjustment of the parameters we arrived at a set of values in Table 3, which matches the bifurcation behavior of the system as close as possible. Our guidelines for finding the “optimal” values were the location and shape of regions with specific dynamical regimes and the position of a crossover point, where the region of coexisting steady states SS I and SS II meets the region of oscillations. In general, by setting  $k_6$  and  $k'_6$  to lower values all the domains are shifted to lower values of  $k_0$ . On the other hand,  $k_2$  and  $k_3$  affect the position of the crossover point.

The numerically obtained bifurcation diagram in the  $k_0$ – $c_0(\text{S}_2\text{O}_3^{2-})$  parameter plane (Figure 2) is delineated by two Hopf bifurcation curves (HB) marking the onset of oscillations

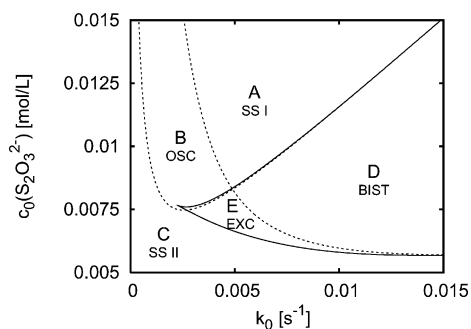


**Figure 2.** Numerically calculated bifurcation diagram in the parameter plane  $k_0$ – $c_0(\text{S}_2\text{O}_3^{2-})$ . Conditions:  $c_0(\text{H}_2\text{O}_2) = 0.1$  mol/L,  $c_0(\text{H}^+) = 0.002$  mol/L,  $c_0(\text{Cu}^{2+}) = 2.5 \times 10^{-5}$  mol/L. Key: dashed line, Hopf bifurcation curve; full line, saddle-node bifurcation curve. Labels: OSC, oscillations; BIST, bistability between SS I and SS II; EXC, stable but excitable SS II and unstable SS I.

and a cusp-shaped saddle-node bifurcation curve (SNB) where two steady states merge. The structure is of a cross-shape type, even though strongly asymmetric. The curves partition the parameter space into five main regions corresponding to distinct dynamical modes. In region A bounded by the HB curve on the left and by the SNB curve on the right, there is only one stable steady-state SS I with a basic pH. The adjacent oscillatory region B is located between the HB curves to the left and above their intersection, which constitutes the crossover point. In region C, unique weakly acidic stable steady-state SS II occurs. Inside the cusp-shaped SNB curve three steady states coexist, SS I, SS II and a (always unstable) saddle point; in region D both SS I and SS II are stable, in region E only SS II is stable. Such a bifurcation structure suggests that excitability may occur in region E (also in region C close to region E) and, possibly, in region A close to the crossover point.<sup>21</sup> By comparison of the experimental and calculated bifurcation diagrams, the most striking difference is the absence of the region of coexisting oscillations and SS I in the model. Also, the tilt of the region of multiple steady states and the extent of the oscillatory region are inconsistent. This evidence already suggests that the model is far from complete, which is further corroborated by our pulse experiments and summarized in the discussion.

### 3. Experiments with External Pulses

Experiments with external pulses were carried out in a CSTR with the volume of 18.2 mL and magnetic stirring (25 Hz). Feed solutions were delivered with the use of a peristaltic pump (Ismatech). The solutions were prepared daily from highest grade commercially available chemicals ( $\text{H}_2\text{O}_2$ ,  $\text{Na}_2\text{S}_2\text{O}_3 \cdot 5\text{H}_2\text{O}$ ,  $\text{CuSO}_4 \cdot 5\text{H}_2\text{O}$ ,  $\text{H}_2\text{SO}_4$ , NaOH) with the use of deionized water. Required temperature of 25 °C was maintained via a thermostat (Haake). The reactor had a metal bottom to ensure rapid heat exchange with the coolant (deionized water). Temperature and pH in the reactor were monitored during experiments by means of a platinum resistance thermometer (Pt100) and a glass combined semi-micro pH-electrode (Theta), respectively. The signals from the sensors were amplified, digitized, processed and stored in a computer. Pulsed additions of reactants were done via a syringe pump. The entire data flow was controlled within the LabVIEW programming environment.

The experiments with pulsed additions of a perturbant to the reactor were done mostly at the weakly acidic steady-state SS II for values of external constraints close to transition to oscillations, where the steady-state SS II was deemed excitable ( $c_0(\text{H}_2\text{O}_2) = 0.1$  mol/L,  $c_0(\text{S}_2\text{O}_3^{2-}) = 0.008$  mol/L,  $c_0(\text{H}_2\text{SO}_4) = 0.001$  mol/L,  $c_0(\text{Cu}^{2+}) = 2.5 \times 10^{-5}$  mol/L,

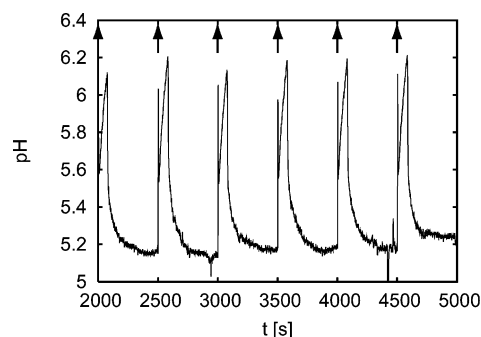


**Figure 3.** Experimental pH trace of the dynamical response to periodic perturbations of SS II by  $\text{OH}^-$ . Conditions:  $c_0(\text{H}_2\text{O}_2) = 0.1$  mol/L,  $c_0(\text{S}_2\text{O}_3^{2-}) = 0.008$  mol/L,  $c_0(\text{H}_2\text{SO}_4) = 0.001$  mol/L,  $c_0(\text{Cu}^{2+}) = 2.5 \times 10^{-5}$  mol/L,  $k_0 = 0.0045$  s<sup>-1</sup>,  $T = 500$  s,  $\Delta c(\text{OH}^-) = 2.4$  mmol/L. In this and subsequent figures, the arrows pointing up/down indicate the instants of pulsed additions and initial increase/decrease of pH.

$k_0 \approx 0.0045$  s<sup>-1</sup>). Some experiments were done at the weakly basic steady-state SS I and also at a periodic oscillatory regime that emerges from SS II via a Hopf bifurcation when  $k_0$  is decreased. In each experiment, the flow rate was kept fixed and timing of the syringe pump was controlled. The time duration of injection (typically a few seconds) was used as a control parameter of the amount of perturbant added. The amplitude of the perturbation  $\Delta c$  was defined as the amount of moles added per unit volume of the reacting mixture and the time between pushes of the syringe determined the period of forcing  $T$ . Under these conditions, the system was perturbed by adding certain amounts of NaOH,  $\text{H}_2\text{SO}_4$ ,  $\text{S}_2\text{O}_3^{2-}$ ,  $\text{SO}_3^{2-}$ , and  $\text{S}_4\text{O}_6^{2-}$ . These experiments with pulsed additions of chemical species were done in two ways. First, a perturbation was repeated with a sufficiently long period so that the response was allowed to return to the steady state and at the next pulse the amplitude of the perturbation was increased. This arrangement served for finding conditions under which the system begins to respond by excitation, and also conditions under which the excitability vanishes. Next, we chose appropriate amplitude of perturbation and carried out a series of periodic forcing experiments with fixed amplitude and successively varying forcing period.

**Perturbations by Base.** If the system is in the weakly acidic steady-state SS II ( $k_0 = 0.0045$  s<sup>-1</sup>), a supercritical pulse of base (NaOH) invokes a very sharp spike lasting a few seconds followed by a broader peak corresponding to an accumulation of hydroxide ions within several tens of seconds and later their depletion within a few hundreds of seconds until the steady state is reestablished (Figure 3). We characterize the response dynamics as excitatory, because each spike associated with the pulse is followed by a self-amplifying signal with maximum exceeding the height of the spike. A similar dynamic feature is also present for a lower flow rate  $k_0 = 0.0027$  s<sup>-1</sup> where the excitable SS II is replaced by a periodic oscillatory regime with the spontaneous oscillatory period  $T_p \approx 500$  s. For medium periods of forcing (from 200 to 300 s) this forced oscillator even shows a subharmonic period-two pattern with two alternating double-peaks (Figure 4). The larger of the two responses can be seen as excitatory, whereas the smaller one is a case of marginal excitability, where the peak following the spike is rather small and narrow. Subharmonic regimes were observed also for larger  $k_0$  where the steady state is stable and excitable.

**Perturbations by Acid.** At the weakly acidic steady-state SS II for the same value of  $k_0 = 0.0045$  s<sup>-1</sup>, the pulse of acid ( $\text{H}_2\text{SO}_4$ ) causes the system to drop its pH proportionally to the amount of added acid, but after passing through a shallow minimum taking a few hundreds of seconds, pH starts to grow



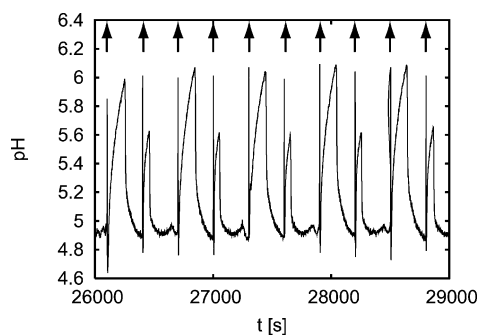


**Figure 4.** Experimental pH trace of the dynamical response to periodic perturbations of oscillations by  $\text{OH}^-$ . Conditions:  $c_0(\text{H}_2\text{O}_2) = 0.1$  mol/L,  $c_0(\text{S}_2\text{O}_3^{2-}) = 0.008$  mol/L,  $c_0(\text{H}_2\text{SO}_4) = 0.001$  mol/L,  $c_0(\text{Cu}^{2+}) = 2.5 \times 10^{-5}$  mol/L,  $k_0 = 0.0027$  s $^{-1}$ ,  $T = 300$  s,  $T_p = 500$  s,  $\Delta c(\text{OH}^-) = 1.2$  mmol/L.

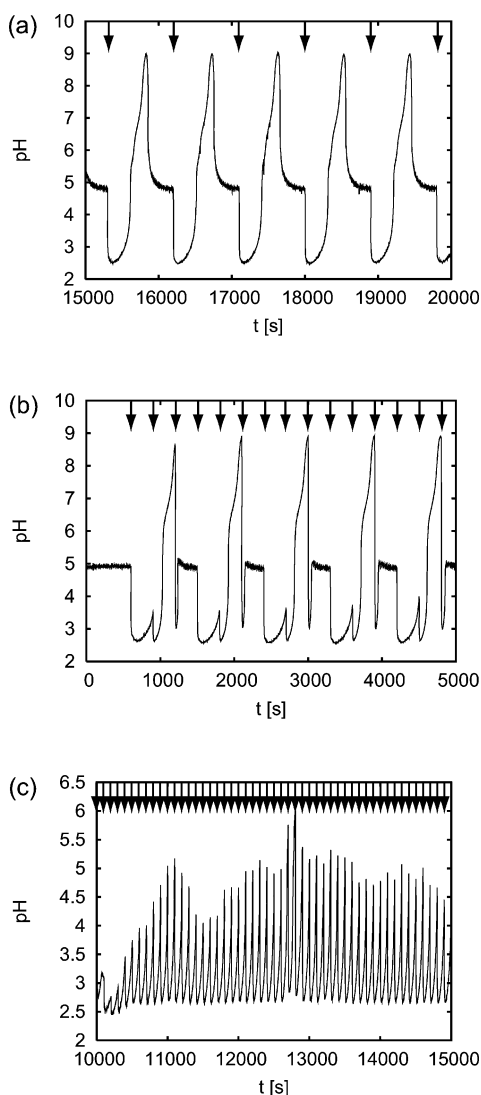


**Figure 5.** Experimental pH traces of the dynamical response to periodic perturbations of SS II by  $\text{H}^+$ : (a)  $T = 900$  s, (b)  $T = 300$  s, (c)  $T = 100$  s. Conditions:  $c_0(\text{H}_2\text{O}_2) = 0.1$  mol/L,  $c_0(\text{S}_2\text{O}_3^{2-}) = 0.008$  mol/L,  $c_0(\text{H}_2\text{SO}_4) = 0.001$  mol/L,  $c_0(\text{Cu}^{2+}) = 2.5 \times 10^{-5}$  mol/L,  $k_0 = 0.0045$  s $^{-1}$ ,  $\Delta c(\text{H}^+) = 2.4$  mmol/L.

rapidly (Figure 5a). During this process the concentration of  $\text{H}^+$  ions decreases by 6 orders of magnitude. After reaching the maximum at about 9 units of pH, the system relaxes very rapidly to the steady state. Thus the addition of acid surprisingly leads to a huge overshoot in the response, which is a manifestation of a strong and quite peculiar excitability. If the system in

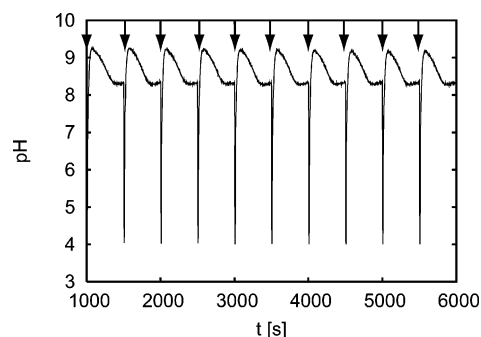


**Figure 6.** Experimental pH trace of the dynamical response to periodic perturbations of SS I by  $\text{H}^+$ . Conditions:  $c_0(\text{H}_2\text{O}_2) = 0.1$  mol/L,  $c_0(\text{S}_2\text{O}_3^{2-}) = 0.012$  mol/L,  $c_0(\text{H}_2\text{SO}_4) = 0.001$  mol/L,  $c_0(\text{Cu}^{2+}) = 2.5 \times 10^{-5}$  mol/L,  $k_0 = 0.0053$  s $^{-1}$ ,  $T = 500$  s,  $\Delta c(\text{H}^+) = 7.2$  mmol/L.

the steady-state SS II is forced periodically with period in a medium range (from 200 to 500 s), there is not enough time to complete the overshoot and various resonant response patterns are observed. In Figure 5b, the system responds periodically with one complete cycle per three external pulses. Only every third response is an excitation as the system is refractory when responding to pulses applied at a dynamical state well away from the steady state. Very short forcing periods lead to a pattern of dense spikes of small amplitudes (Figure 5c). We ascribe such dynamics to quasiperiodicity with slowly varying maxima in the range from 4 to 6 pH units, which only occasionally overshoot the steady-state value at  $\text{pH} \approx 5$ . Experiments with periodic forcing by acid applied to the oscillatory regime show similar resonant responses as the forced steady state.

Next we examined excitability of the system at the basic steady-state SS I. We found that if the system is perturbed by acid, the return to SS I produces slight overshoots of about 1 pH unit (Figure 6). Maxima of the overshooting peaks at  $\text{pH} \approx 9$  are consistent with those in Figure 5a,b suggesting that the same chemical process is in operation. Periodic perturbations did not have any influence on the amplitude of oscillations and the response dynamics was always 1:1 synchronized with the external pulses. In addition, we observed that in the region of bistability between the weakly acidic SS II and the weakly basic SS I, it is possible to switch between the steady states by addition of acid.

**Perturbations by Other Species.** With the use of  $\text{S}_2\text{O}_3^{2-}$  as perturbant, we detected an excitatory response only for SS II (Figure 7a). A superthreshold addition of  $\text{S}_2\text{O}_3^{2-}$  induces amplification of pH to values that spontaneously exceed the level corresponding to the pulse itself ( $\text{pH} \approx 6$ ). This excitability is akin of that when the SS II is perturbed by base (Figure 3). Remarkably, for forcing periods equal to 250 and 200 s we observed a bistability between two oscillatory regimes (Figure 7b), which was well reproducible. One of these forced oscillators is corresponding to the perturbed SS II, the second one oscillates in a weakly basic range 8–9 pH around SS I. When the perturbations are applied to the regime of spontaneous oscillations (at lower flow rates) the system readily synchronizes with external pulses and the waveform of the oscillations is similar to that of the forced excitable system. Under these conditions no bistability of dynamical regimes was found. By perturbing the weakly basic steady-state SS I with  $\text{S}_2\text{O}_3^{2-}$ , we did not find any excitability. In other series of experiments we examined the response of the system to pulsed additions of  $\text{S}_4\text{O}_6^{2-}$  and  $\text{SO}_3^{2-}$ . However, the system did not show any excitatory response.

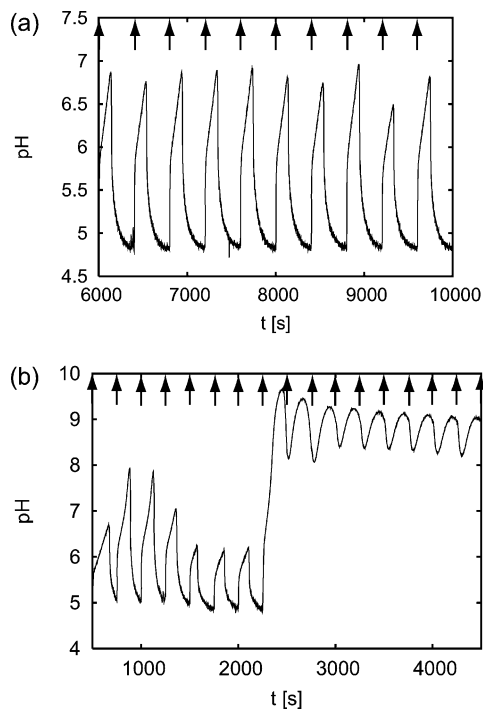


**Figure 7.** Experimental pH traces of the dynamical response to periodic perturbations of SS II by  $\text{S}_2\text{O}_3^{2-}$ . Conditions:  $c_0(\text{H}_2\text{O}_2) = 0.1$  mol/L,  $c_0(\text{S}_2\text{O}_3^{2-}) = 0.008$  mol/L,  $c_0(\text{H}_2\text{SO}_4) = 0.001$  mol/L,  $c_0(\text{Cu}^{2+}) = 2.5 \times 10^{-5}$  mol/L,  $k_0 = 0.0055$  s $^{-1}$ ,  $\Delta c(\text{S}_2\text{O}_3^{2-}) = 4.8$  mmol/L. (a)  $T = 400$  s, (b)  $T = 250$  s.

#### 4. Calculations with External Pulses

The model of the system described by eqs 1 with optimized parameters (Table 3) was used to simulate the response of the perturbed system. The pulsed forcing is provided by periodically repeated jump-wise increase of the actual concentration of the perturbed chemical species by an amplitude  $\Delta c$  in the course of numerically solving the model. In the search of conditions for excitable dynamics in simulations, we were guided on the one hand by the computed bifurcation diagram (Figure 2), which indicates an excitable steady-state SS II at parameters corresponding to the region E and adjacent region C, and possibly excitable SS I in region A, on the other hand by experimental response curves, which we tried to match as closely as possible. Consequently, the bifurcation parameters  $k_0$  and  $c_0(\text{S}_2\text{O}_3^{2-})$  depart somewhat from the experimental ones in order to maintain the steady-state pH close to the experimental values.

Suprathreshold periodic pulsed additions of hydroxide ions to the system at SS II with the forcing period  $T = 500$  s cause dynamical responses (Figure 8), which are qualitatively comparable to the measured ones (Figure 3). As in the experiment, the calculated waveform includes a narrow spike followed by a broad and large peak. However, the simulations display responses ranging between 4 and 10 pH units and thus are substantially larger than the experimental results show. Also, after the pulse causing the large amplitude excitatory response in Figure 8, the following pulse is applied at the instant, when pH undershoots the steady-state value ( $\text{pH} \approx 5.5$ ) and so the perturbation is absorbed by the system as it continues in relaxation toward the steady state. In contrast, experiments in Figure 3 show excitatory response to every pulse. This is because the refractory period is longer in the model and thus only every second perturbation causes an excitation unlike in the experiment. On the other hand, experiments with forced periodic oscillations shown in Figure 4 do show subharmonic entrainment, which appears due to the significantly shorter

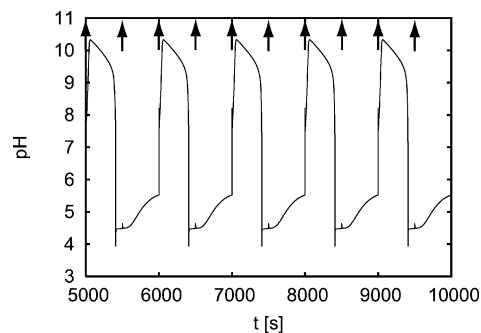


**Figure 8.** Calculated pH trace of the dynamical response to periodic perturbations of SS II by  $\text{OH}^-$ . Conditions:  $c_0(\text{H}_2\text{O}_2) = 0.1$  mol/L,  $c_0(\text{S}_2\text{O}_3^{2-}) = 0.008$  mol/L,  $c_0(\text{H}^+) = 0.002$  mol/L,  $c_0(\text{Cu}^{2+}) = 2.5 \times 10^{-5}$  mol/L,  $k_0 = 0.005$  s $^{-1}$ ,  $T = 500$  s,  $\Delta c(\text{OH}^-) = 0.01$  mmol/L.

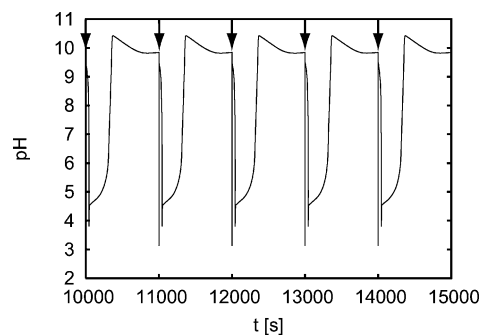


**Figure 9.** Calculated pH trace of the dynamical response to periodic perturbations of SS I by  $\text{H}^+$ . Conditions:  $c_0(\text{H}_2\text{O}_2) = 0.1$  mol/L,  $c_0(\text{S}_2\text{O}_3^{2-}) = 0.01$  mol/L,  $c_0(\text{H}^+) = 0.002$  mol/L,  $c_0(\text{Cu}^{2+}) = 2.5 \times 10^{-5}$  mol/L,  $k_0 = 0.005$  s $^{-1}$ ,  $T = 1000$  s,  $\Delta c(\text{H}^+) = 0.75$  mmol/L.

forcing period  $T = 300$  s relative to the autonomous period  $T \approx 500$  s (consistent results are obtained in simulations).

If SS II under the same external constraints as in the experiments is perturbed by a pulsed addition of acid, then initially pH of the system drops instantaneously and from this value the pH rises monotonously to the value corresponding to the steady state (not shown). Thus, in contrast to the experiments (Figure 5a,b), the model does not exhibit excitable dynamics.

External additions of acid to the weakly basic steady-state SS I with  $\text{pH} \approx 9.5$  (Figure 9) cause an immediate drop to  $\text{pH} \approx 3$ , which returns very rapidly ( $t \approx 0.1$  s) to the basic range forming thus an inverse spike and then a large-amplitude well-developed trough follows, terminated by an overshoot of the steady-state pH. This dynamics involves spontaneous accumulation and later depletion of hydrogen ions, which signifies excitatory dynamics. This dynamical behavior somewhat resembles the corresponding experimental dynamics (Figure 6), particularly the overshoot part. However, there does not seem to be any spontaneous decrease of pH preceding its recovery in the experiments, only a direct rapid return to the basic range of pH.

The last series of calculations was done with pulsed additions of sulfur compounds: thiosulfate, tetrathionate, and sulfite. Pulsed additions of these species are expected to affect the dynamics of the model because of their role as important reactants/intermediates in the mechanism. Dynamics forced by thiosulfate and sulfite copy the oscillatory response of the system perturbed by base as shown in Figure 8, whereas pulsed additions of tetrathionate do not show any significant effect.

#### 5. Discussion

Due to its complex mechanism, the  $\text{H}_2\text{O}_2$ – $\text{S}_2\text{O}_3^{2-}$ – $\text{H}_2\text{SO}_4$ – $\text{Cu}^{2+}$  reaction displays a rich variety of dynamical regimes

including three different steady states, simple periodic and mixed-mode periodic oscillations,<sup>9</sup> and recently reported mixed-mode chaotic and quasiperiodic regimes.<sup>22</sup> When arranged into bifurcation diagrams as presented by Orbán and Epstein<sup>9</sup> and in this work, the regions of steady states and oscillations form a structure partly resembling a cross-shaped diagram. We used the mechanism proposed by Kurin-Csörgei et al.<sup>17</sup> and optimized the values of adjustable parameters by successively constructing bifurcation diagrams with the aim of achieving best possible agreement with experiments. Superficially, our attempt seemed fairly successful, but simulations of experimental time series for the periodically pulsed system show significant discrepancies.

In our experiments on the response of the system to pulsed additions of chemical species applied to different steady states and oscillations we discovered several cases for which the responses of the system to pulsed additions of certain species are excitatory. When the period of forcing was sufficiently short, we observed subharmonic responses due to refractoriness of the system and for very short forcing periods also quasiperiodic small-amplitude oscillations.

Responses of the system to external pulses of the two obvious key species for pH oscillators, the hydrogen and hydroxide ions, are quite intriguing. The system at the weakly acidic steady-state SS II is excitable with respect to both of these species. Because of their rapid association to form water, they are expected to play opposite roles in the mechanism, which would seem to imply excitability with respect to adding one of the species only. However, both perturbants imply an eventual rapid increase in pH, which would seem to suggest that  $\text{OH}^-$  is the autocatalytic species. Another remarkable feature is that the steady-state value of  $\text{pH} \approx 5$  rises to very different levels in the two cases; perturbation by base causes an increase to  $\text{pH} \approx 6$ , and perturbation by acid evokes a peak with a maximum at  $\text{pH} \approx 9$ . Apparently, there are two different reaction pathways involved in these two kinds of responses. A closer look at Figure 5a,b reveals that the increase of pH after a pulse of acid proceeds in two phases, the first one, from  $\text{pH} \approx 3$  to  $\text{pH} \approx 6$ , is faster than the following phase terminating at  $\text{pH} \approx 9$ , which suggests two different dominant processes to take place. By its pH range, the first phase corresponds to the response observed in the experiments with perturbation by base (Figures 3 and 4). It seems to indicate that the first process is the  $\text{OH}^-$  autocatalysis occurring when either of the perturbants is used, and the second process is a peculiar additional feature activated only when acid is the perturbant. However, these observations do not rule out  $\text{H}^+$  as being the autocatalytic species. Based on activatory (autocatalytic) and inhibitory processes that form a chemical oscillation, there are two possible excitatory responses,<sup>23</sup> *activatory* or *inhibitory*, depending on whether the concentration of the autocatalytic species at the steady state is at a low or high level, respectively. In the activatory case, the perturbation causes the autocatalytic process to start first, followed by the inhibitory process causing eventual relaxation to the steady state. In the second case, it is the inhibitory process that is initiated first, followed by the activatory process that replenishes the autocatalytic species. Thus if  $\text{H}^+$  were the activator at a high steady-state level, which is consistent with SS II, then the increase of pH upon the perturbation would represent the inhibitory process followed by the autocatalytic drop of pH. Conversely, if  $\text{OH}^-$  were the activator at a low level, which is also consistent with SS II, then inhibition and autocatalysis are reversed. Therefore further experimental clues are needed.

One may suspect that the initial spike of the response to every perturbation of SS II by base (Figures 3 and 4) is a consequence of insufficient stirring rather than kinetics. We checked the dynamics by a dummy experiment, where the base was injected into the reactor fed with pure water. The pH of the system rose up immediately after injection of hydroxide and then it dropped gradually as the reactor contents were eluted by inflowing water. We conclude that the spike has its origin in kinetics, which is presumably governed by rapid protonation-deprotonation equilibria. Another spike-related question is an operational definition what constitutes an excitatory response. We consider the whole spike as a perturbation combining the pulsed addition itself and a fast equilibration, which almost instantaneously shifts the pH of the system by a few tenths. The subsequent response reflecting activatory/inhibitory kinetics is thought as excitatory if its amplitude exceeds the pH change caused by the pulse. Even with this definition, the excitability by adding base (Figure 3) is quite weak when compared with that by adding acid, where the response amplitudes are huge relative to the size of perturbations (Figure 5a,b). The system is also weakly excitable at SS II with respect to perturbations by thiosulfate (Figure 7a).

Response to perturbations of the weakly basic steady-state SS I by acid may also be considered as excitable (Figure 6) with the initial spike being inverse and the response overshooting the concentration of hydroxide ions at the steady state by an order of magnitude. This peak is apparently related to the second aforementioned process.

Simulations of the dynamics when the system is perturbed by base at SS II (Figure 8) show a very rapid growth of pH to a maximum value of 10.5 followed by a drop with an undershoot of the steady-state pH level, whereas perturbation by acid does not generate excitation. In the mechanism, the first step assumes  $\text{Cu}^{2+}$  catalyzed autocatalysis in  $\text{OH}^-$  (Table 1), which likely accounts for the observed rapid pH increase. In experiments, the increase should stop at  $\text{pH} \approx 6$  while the simulated pH continues to grow. In fact, this happens in the experiments with the perturbation by acid, though the slowing down of the rate of pH growth above  $\text{pH} \approx 6$  is absent in the calculated curve. The observed dynamics of the model is a manifestation of the activatory excitability. The weakly basic steady-state SS I can be perturbed by acid to obtain an excitatory response (Figure 9), which, however, has a somewhat different course than the experiment (Figure 6). Following the spike, there is a decrease of pH before the peak overshooting the steady-state pH level occurs. Such dynamics of the model correspond to the inhibitory excitability. But the corresponding experimental curve does not support such an interpretation.

Discrepancies between simulated and measured results are on a quantitative level for base and thiosulfate perturbations but on a qualitative level for acid and sulfite perturbations. An open problem remains whether this system is a pH or rather a pOH oscillator. Our experiments with excitable dynamics can be interpreted either way. Typically, the autocatalytic process is much faster than the complementary inhibitory process. Based on the experiments, the  $\text{H}^+$  autocatalytic process would seem more appropriate because the decrease in pH is significantly faster than its increase. In contrast, the mechanism is based on  $\text{Cu}^{2+}$  catalyzed autocatalysis of hydroxide ions. Additionally, there are several other sources of autocatalysis in the mechanism.<sup>8</sup> Yet it does not seem that they can be combined by adjusting kinetic parameters to reproduce the experiments. More likely, there are some missing parts.<sup>24</sup> Hence, a more detailed analysis of the mechanism is needed to settle this question, and

apart from kinetic measurements, special tools such as the classification of oscillatory reactions may be employed.<sup>25</sup>

**Acknowledgment.** We thank M. Orbán for helpful discussions. This work has been supported by the grant from the Czech Science Foundation No. GACR 203/06/1269 and the project from the Czech Ministry of Education No. MŠMT 6046137306.

## References and Notes

- (1) Field, R. J.; Burger, M. *Oscillations and Travelling Waves in Chemical Systems*; Wiley: New York, 1985.
- (2) Epstein, I. R.; Kustin, K.; De Kepper, P.; Orbán, M. *Sci. Am.* **1983**, *248*, 112.
- (3) Orbán, M.; Epstein, I. R. *J. Am. Chem. Soc.* **1985**, *107*, 2302.
- (4) Rábai, G.; Orbán, M.; Epstein, I. R. *Acc. Chem. Res.* **1990**, *23*, 258.
- (5) Luo, Y.; Epstein, I. R. *J. Am. Chem. Soc.* **1991**, *113*, 1518.
- (6) Frerichs, G. A.; Thompson, R. C. *J. Phys. Chem. A* **1998**, *102*, 8142.
- (7) Rábai, G.; Nagy, Z. V.; Beck, M. T. *React. Kinet. Catal. Lett.* **1987**, *33*, 23.
- (8) Rábai, G.; Hanazaki, I. *J. Phys. Chem. A* **1999**, *103*, 7268.
- (9) Orbán, M.; Epstein, I. R. *J. Am. Chem. Soc.* **1987**, *109*, 101.
- (10) Kovács, K. M.; Rábai, G. *J. Phys. Chem. A* **2001**, *105*, 9183.
- (11) Vanag, V. K. *J. Phys. Chem. A* **1998**, *102*, 601.
- (12) Hauser, M. J. B.; Strich, A.; Bakos, R.; Nagy-Ungvarai, Z.; Müller, S. C. *Faraday Discuss.* **2001**, *120*, 229.
- (13) Orbán, M.; De Kepper, P.; Epstein, I. R. *J. Phys. Chem.* **1982**, *86*, 431.
- (14) Rábai, G.; Beck, T.; Kustin, K.; Epstein, I. R. *J. Phys. Chem.* **1989**, *93*, 2853.
- (15) Orbán, M.; Epstein, I. R. *J. Am. Chem. Soc.* **1990**, *112*, 1812.
- (16) Alexander, J. C.; Doedel, E. J.; Othmer, H. G. *SIAM J. Appl. Math.* **1990**, *50*, 1373; Aidley, D. J. *The Physiology of Excitable Cells*; Cambridge University Press: Cambridge, U.K., 1998.
- (17) Kurin-Csörgei, K.; Orbán, M.; Rábai, G.; Epstein, I. R. *J. Chem. Soc., Faraday Trans.* **1996**, *92* (16), 2851.
- (18) Pešek, O.; Kašpar, P.; Schreiberová, L.; Schreiber, I. *J. Phys. Chem. A* **2004**, *108*, 2436.
- (19) Boissonade, J.; De Kepper, P. *J. Phys. Chem.* **1980**, *84*, 501.
- (20) Kohout, M.; Schreiber, I.; Kubíček, M. *Comput. Chem. Eng.* **2002**, *26*, 517.
- (21) Zagora, J.; Voslař, M.; Schreiberová, L.; Schreiber, I. *Phys. Chem. Chem. Phys.* **2002**, *4*, 1284.
- (22) Bakeš, D.; Schreiberová, L.; Schreiber, I.; Hauser, M. J. B. *Russ. J. Phys. Chem. A* **2007**, *81*, 1407.
- (23) Zagora, J.; Voslař, M.; Schreiberová, L.; Schreiber, I. *Faraday Discuss.* **2001**, *120*, 313.
- (24) Voslař, M.; Matějka, P.; Schreiber, I. *Inorg. Chem.* **2006**, *45*, 2824.
- (25) Ross, J.; Schreiber, I.; Vlad, M. O. *Determination of Complex Reaction Mechanisms*; Oxford University Press: New York 2006.